VIP Final report

Team P=NP, Data Dynamics

Wenzhao Wei Peiju Li Zelun Li Yi Zhuang Cristian Bernal Karim Saad

***Abstract*—Cognitive impairment is currently heavily affecting the elderly population. Due to the continual growth of computer vision and artificial intelligence, it is possible to combine this medical problem with existing artificial intelligent algorithms. We applied the Alzheimer's Disease Neuroimaging Initiative (ADNI) dataset to explore the brain connectivities by applying and comparing between several advanced neural network and graph model such as GCN, st-GCN, NN. We achieved 76% accuracy for the predictions of cognitive impairments such as Alzheimer Disease (AD) and Cognitive Normal (CN) state and have shown a step-by-step pathway to achieve these results and explore the problem.**

***Index Terms*—fMRI, Neural Network, Graph Convolution Network, brain functional connectivities**

I. Introduction

Cognitive disorders, which is a general category including conditions such as Alzheimer's disease, mild cognitive impairment, and subjective cognitive decline, usually encompass the disorder of memory, language, visual space, a neurodegenerative disorder that currently affects over 30 million people worldwide [30]. Alzheimer's disease as one of the most common neurodegenerative diseases could gradually damage their memory, language, and behaviours. Due to the slow exhibition of symptoms, the clinic experiments usually have a difficult time identifying it. The cognitive disorders are suggested to be associated with dysfunction of the brain connectivity network and is considered a connectivity disorder. With the swift increment of dementia patients number, a number of recent studies have attempted to diagnose and stage AD using non-invasive image-derived brain connectivity graphs such as fMRI, dMRI and EEG etc[42].

Various open source databases have emerged and accelerated the research in the field. Databases like AIBL(aibl.csiro.au), OASIS(www.oasis-brain.org) are available for academic purposes. We choose ADNI(adni.loni.usc.edu), a relatively new database for our study [50].

The ADNI dataset contains resting-state functional magnetic resonance imaging (rs-fMRI) are non-invasive imaging modalities that measure a blood-oxygen-level-dependent (BOLD) signal that is indicative of neural activity over time, at each voxel. This signal is typically averaged within each region of interest (ROI). The assumption is that the temporal similarity between the BOLD signals in each region as an indicator of synchronous neural activity demonstrates functional connectivities in the human connectome [5]. fMRI appears to be the ideal neuroimaging technique for the investigation of resting-state network characteristics due to its superiority in spatial resolution compared to other methodology such as EEG [36].

A. Recent studies

The advances in computer vision and artificial intelligence have increased the accessibility of these technologies for researchers and clinicians, and have substantially enhanced our understanding of the human brain, improving diagnoses and treatments of neurological disorders. In recent literature, a number of studies incorporating computer vision and artificial intelligence to assist in the early diagnosis of fMRI data has shown great success in terms of its ability to automate AD diagnose and detection. The past few years has seen the growing prevalence of employing machine learning methods for Alzheimer's. Among the vast amount of methods employed by numerous researchers, support vector machines (SVM), artificial neural networks (ANN) and deep learning (DL) are found to be most effective when discovering the underpinning neurological causes of cognitive impairment [44].

1) SVM: Recently SVM has been used in the study of the identification of cognitive impairment patients using fMRI data. In 2016, SVM was used to classify AD and Health Control (HC) based on the discriminating features of hippocampus and amygdaloid volume by Jongkreangkrai et al (2016) [17]. Later studies have managed to increase the accuracy of binary classification between AD and HC using SVM classifier to 92.48% [4]. As mentioned above, SVM has shown a high performance on the binary classification problem.

2) ANN: ANN were employed on tasks relating to this cognitive disorder in a extensive manner, as numerous classification algorithms such as random forest (RF), decision tree, bagging, multilayer perceptron (MLP) were compared by Joshi et al.[18].

3) DL: Deep learning has provided a powerful toolbox for standard-grid like image classification of the brain, however their application on connectome data has been limited due to its complex information composition and the dearth of data volume unlike grid like images [5], [13], [21], [26], [57].

B. Challenge and difficulties

Brain connectome data is unique and complex which present both special challenges and opportunities when used for machine learning [5].

Unlike standard medical images which are gridlike with each pixel neighbouring only other pixels that are spatially

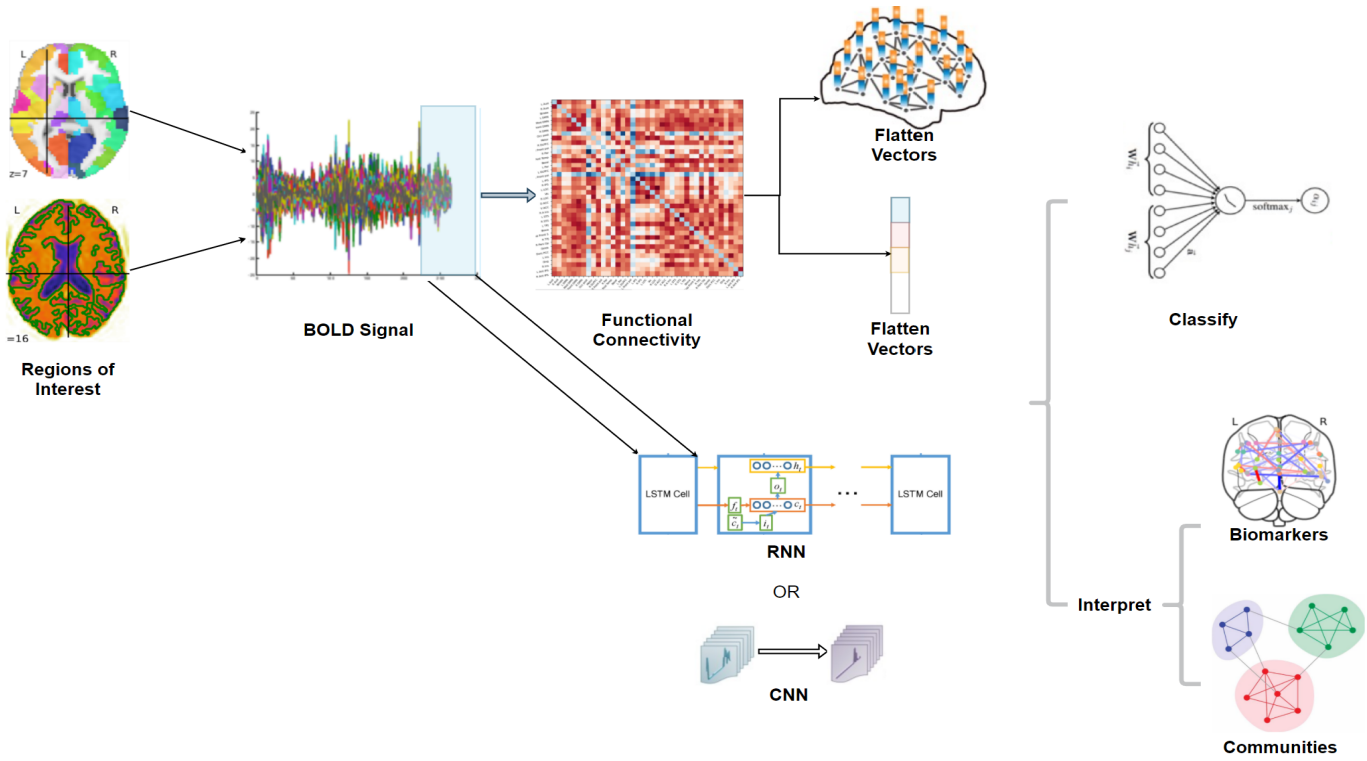

Fig. 1: Generalised Deep Learning Pipeline

nearby, connectomes have a more general topology and temporal features that need to be considered when analysing from fMRI data [5]. Since this measurement is based on the temporal correlation of changes in the functional MRI signal between different parts of the brain, any process that affects the signal and has nothing to do with neural activity will affect the measurement of functional connectivity, which will lead to false results. Potential confounds arising from motion, cardiac and respiratory cycles, arterial CO2 concentration, blood pressure/cerebral auto-regulation, and vasomotion are discussed [36]. Although the data acquisition for fMRI imaging is due to the use of open-source projects like ADNI, ABIDE, ADHD and HCP etc. It is challenging to acquire consistent and large amounts of fMRI data. It exacerbates the high dimension, small sample size issue of the data when used during model training, which often results in the algorithms overfitting this data.

Moreover, the accuracy of the problem is largely variable depending on the type of classification. For instance the accuracy remains the highest for AD vs HC and plummets between MCI and AD. Furthermore, relative to the data set the classification problem can be narrowed to MCI converters (MCIc) versus non-converters (MCInc) or amnestic MCI(aMCI) versus nonamnestic MCI(naMCI)[44]. However, the narrower classification problem has a fundamental barrier, known as the *yo-yo effect*. The *yo-yo effect* relates to the fluctuation of a patients diagnosis in their cognitive ability [61]. The changeability of the diagnosis can lead to a false clinical judgement, hence mitigating the quality of the data obtained.

Therefore, extracting the most distinctive features that contributes to mental disorders is the primary objective of the current study. In our research work, we aim to complement this research gap, while forming an interpretable pipeline for clinicians and the general public to deepen their understanding of human connectomes. During which we will explore the current literature and propose a novel, effective and robust architecture to refine this AD diagnosis pipeline.

II. Preprocess

The data we used was prepared first following the default 9 steps in the SPM preprocessing pipeline. Functional realignment and unwarp, this step addresses the potential susceptibility distortion-by-motion interactions by estimating the derivatives of the deformation field with respect to head movement and resampling the functional data to match the deformation field of the reference image. After correcting the potential distortion by motion, a slice-timing correction is applied on the data to adjust the temporal misalignment between different slices. Potential outlier scans are identified from the observed global BOLD signal as well as the amount of subject-motion in the scanner. After eliminating the potential outliers in the data, functional and anatomical data are normalized into standard MNI space and segmented into grey matter, white matter, and CSF tissue classes using SPM12 unified segmentation and normalization procedure specified in the 2005 paper by Ashburner and John [3].

After formatting the data in a more "readable" format, denoising is necessary to obtain a meaningful connectivity measure by removing physiological, subject motion, and other confounding effects from the BOLD signal. The first major step is to apply a linear regression model to remove the confounding effects in the data. This is done in 4 smaller steps, firstly the potential confounding effect caused by BOLD noise is being removed by applying a one-voxel binary erosion. Secondly, a total of 12 potential noise components are defined from the estimated subject-motion parameters in order to minimize motion-related to BOLD variability. Thirdly, the scrubbing process removes a variable number of noise components to remove any effect of these outliers on the BOLD signal. Lastly a constant and linear BOLD signal trends within each session to reduce the influence of slow trends. After linear regression, temporal frequencies below 0.008 Hz or above 0.09 Hz are removed from the BOLD signal in order to focus on slow-frequency fluctuations while minimizing the influence of physiological, head-motion and other noise sources [54].

III. Data Augmentation

Data augmentation is an important technique when dealing with a limited amount of training data. By the nature of the cumbersome acquisition process of medical imaging data, data in this field typically has a constraint in data volume. However, when the training data is not enough, it will affect the model performance. Thus, data augmentation technique is required [43]. For high-dimensional data, 4-dimensional grayscale medical images, simple data augmentation methods such as scaling, cropping, flipping, and translations may result in a bad result. As we are analyzing the fMRI image, we need to extract the signal from the image and mask it to the region of interest (ROIs). We must try to maintain the integrity of the brain image. Since a window or temporal cluster is a strict subset of the entire set [5], we can perform the data augmentation in the time domain, incorporating the sliding temporal window to extract the dynamic patterns in brain ROI signals. The input data after preprocessing and applied on the masks of ROI is $N_{regions} \times T_{time} \times N_{subjects}$ and the output data of data augmentation is $N_{regions} \times T_{time} \times N_{times,regionsaugmentation} \times N_{subjects}$

A. Consecutive sliding window

Due to Functional Connectivity being our primary research measure, we need to consider the interactions between each ROI. Sliding window is a common technique when analyzing the dynamic characteristics [56]. We assume that at a given time-stamp, connectivity can be estimated by the span of slices from the time-series data. We can say this operation aims to shorten the time points and extend the sample size.

Figure 2 shows an example of the method, we have 100 time frames and 5 stride gaps between each. In order to find the best window size for the sliding window, while taking into account the dynamics and independence of the data, and keeping as many features as possible, we test different window sizes on the preprocessed raw data.

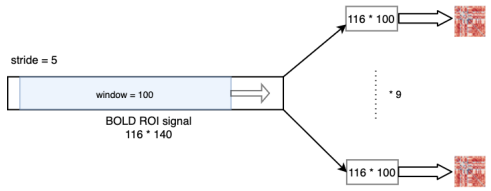

Fig. 2: consecutive 100 time frame

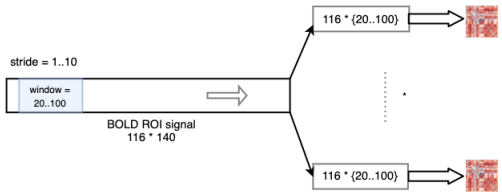

Fig. 3: 20 to 100 window size 2-10 stride size

B. interpolating frames

In this data augmentation technique, the window size and stride have different meanings compared to section III-A. We can reformat a new frame by combining every N frames and the functional dynamic value of new time-stamp is taken as the mean/max of size M windows. The advantage of this method is it can make sure when forming every new image, the whole time interval is considered. It can be used to maintain the consistent effects while increasing the number of samples.

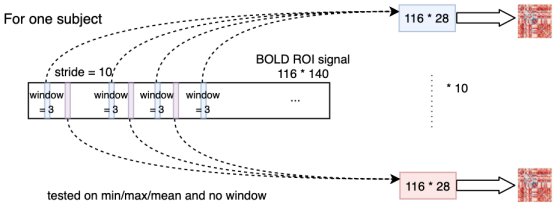

Fig. 4: interpolation method

Figure 4 explains when we have stride numbers of 10, window size as 3, we take 3 frames from every 10 frames, and take the mean or max value of that three frames.

IV. Methods

A. Information extraction

Data extraction on 4d fMRI images aims to reduce the dimensionality from 4D spaces and focus on the functional connectivity of the brain organizations. The regions of interest (ROIs) define sparse representation of brain functional atlases based on macro-anatomical features, cytoarchitecture, functional activations, and/or connectivity patterns and are usually computed based on a predefined atlas or a parcellation scheme [5]. The parcellated brain regions were used as target ROIs to

derive the input connectivity features at the voxel level. Each atlas was used to define a corresponding connectivity matrix computed using Pearson correlation which was fed as input to each model as shown in figure 5. The choice of ROIs can have a significant impact on downstream analysis.

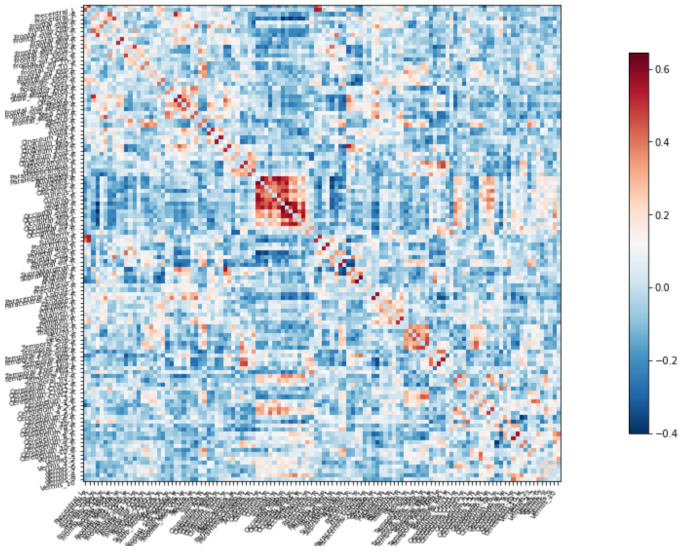

Fig. 5: Functional connectivity matrix derived from brain ROIs based on correlation

In the following sections, we employed both hand-engineered regions of interest (ROIs) based on biomarkers in section IV-A1 and parcellations based on network topological measures of clustering, modularity, small-worldness or segregation in section IV-A2.

1) Biomarkers ROIs: A brain atlas is an anatomical diagram of the brain, split into several different sections. These sections are typically distinguished by various anatomical planes. These diagrams are contiguous and comprehensive, produced as a result of brain mapping. In this project, brain images that are damaged/abnormal will occur frequently, which is why a thorough mapping of the brain is required. The three dimensions that are used to represent the brain imaging are latero-lateral, dorso-ventral and rostral-caudal. The corresponding sections are coronal, sagittal and transverse. The following atlases were explored in this project.

1) AAL [47]
2) MSDL [48]
3) Harvard-Oxford

Note, they all include fMRI data, as per the data we are working with.

Assume we have N subjects, M number of region of interests depends on the masks we are applying on BOLD signals, along T time frames. Then we can form $N * M * M$ time series which are correlated with one to another to determine connectivity among the different ROIs. Which we can get $N * M * M$ functional connectivities value. Since symmetric, we can only use the upper triangular values and then we flatten it to $N * \frac{1}{2} * M * M$ functional connectivities as input.

2) Data Driven Parcellation - Ward Clustering and ICA: Data-driven techniques were employed to generate our brain parcellations in place of brain atlases which we would then use for the down-stream tasks.

Ward Clustering is a criterion applied in hierarchical cluster analysis. In this type of analysis, each point begins as a singular cluster, then the two nearest clusters are gradually merged until either every point is clustered together or until a cluster threshold is reached. For our purposes, fMRI voxels were recursively merged to form clusters throughout the 3D spatial brain image with similar BOLD signals that would form our data-driven ROIs. This technique has been successfully employed previously and had the tendency to outperform other similar clustering methods such a k-means [46].

Ward's clustering employs a distance measure that aims to reduce the total within-cluster variance [14]. At each step of the clustering analysis, each pair of clusters is considered to be merged and the centroid of the new cluster is determined. Then the sum of the squared deviations of all the points within the cluster to this estimated centroid is calculated. This process is repeated for each pair of clusters currently in the data, and the selection for which clusters to merge is determined as the one with the smallest deviation from the new centroid.

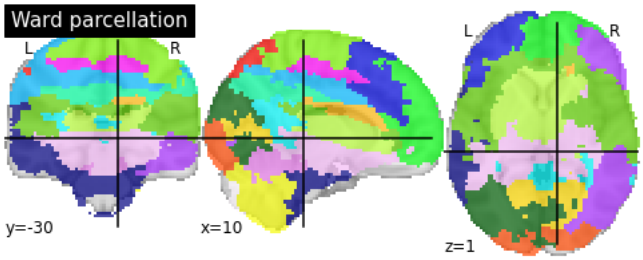

Fig. 6: Ward Clustering with 20 ROIs

The plot in fig 6 shows one of the resulting parcellations generated using Ward Clustering with a clustering threshold of 20.

Blind signal separation involves the separation of a set of source signals from a set of mixed signals without any information regarding the mixing process or the source signals themselves [7]. Independent Component Analysis (ICA) is a family of techniques that are utilised for blind signal separation which assumes that the signals are statistically independent of one another. The diversity of the sources of fMRI data indicates that ICA may be effective in generating our desired brain parcellations in a manner that is data-driven [34], through the identification of independent sources that share similar BOLD signals across time. Previously, ICA has been successfully used in such a way by McKeown and colleagues [33]. We aimed to employ ICA similarly, with group-level analysis of our fMRI dataset using a well-controlled group model, as well as a thresholding algorithm controlling specificity and sensitivity with an explicit model of the signal [52].

The resulting parcellation in fig 7 represents one of the resulting ICA component sets determined by this method.

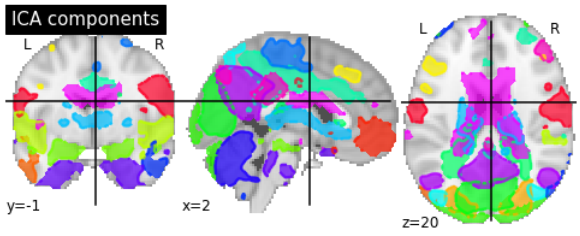

Fig. 7: ICA components with 20 ROIs

Using this spatial map as well as that seen in fig 6, functional connectomes can be generated as seen in fig 8.

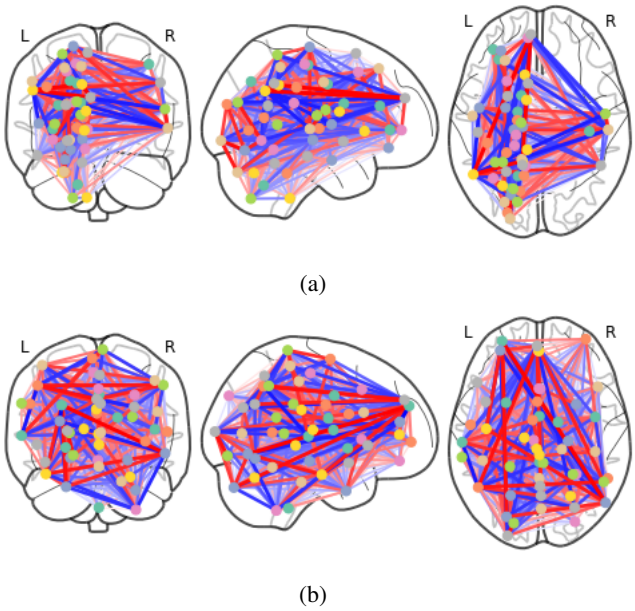

Fig. 8: (a) shows the connectome generated from the ward clustering technique using a 50 cluster threshold. (b) shows the connectome generated from ICA parcellation using a 50 component threshold

B. SVM

A support vector machine (SVM), proposed by Vapnik and his colleagues [9], is a supervised learning model that can classify data with higher dimensionality robustly. The performance of an SVM is largely determined by a few parameters, and thus justifies the results obtained in this project. SVM typically performs better in higher dimensionality spaces and usually has better memory efficiency than deep learning models. Due to a large number of features available, the dimensionality can be quite high in this case. SVM performs better with a clean margin of separation between classes, and performs poorly when the data set is very noisy (i.e. overlapping target classes). The data gathered in this project was done under strict medical conditions, and as such, there is less room for noise.

Previously, SVM has been used on other fMRI classification task for disease diagnosis and metabolic state recognition[12], [62], [20]. In particular, [20] uses SVM on connectivity measures explained in the section above, and this will be used as a benchmark method in this project compared to other deep learning models. Apart from that, SVM performs better where the number of dimensions is greater than the number of samples. In this project, there are approximately 116 dimensions (associated with each feature), and around 300 samples (following denoising). Thus, the SVM will slightly underperform in this case.

C. Spatial Feature Extraction

SVM based multivariate pattern analysis (MVPA) has delivered promising baseline performance in decoding specific brain states based on fMRI brain imaging data [53]. Conventionally, the MVPA based methods heavily relied on feature selection/extraction to prevent overfitting [5].

Convolutional Neural Network (CNN), as the most outperformed architecture in medical image processing [28], has superiority in representing spatial patterns with huge variability and dealing with large noises. A functional CNN majorly consists of three types of layers: convolution layer, pooling layer and fully connected layer [19]. The objective of the convolution layer is to detect and aggregate local conjunctions of spatial features using multiple learnable kernels. These kernels act as filters to extract the pixel-level features at different positions in the input data maps. The idea of using convolution layer is based on the fact that the local groups of pixels are highly correlated and are invariant to locations. By performing convolution operation over these features, the convolution layer generates a multi-channel of 3D features from fMRI images.

A pooling layer is appended after the convolution layer, it performs down-sampling to convert feature images of the preceding convolution layer to lower-dimensions. Max-pooling and Average-pooling are the most common techniques to reduce the number of parameters, by simply taking the largest or average value of surrounding pixels, it can effectively summarise the strongly activated feature abstraction over neighbourhoods.

Fully connected layer and output layer as the last component in the overall CNN framework aims to transform and flatten the well-extracted features, through a fully connected layer to therefore perform the classification task.

Furthermore, both 2D and 3D Convolution can be used on fMRI modal [40]. Classical 2D-centric focuses on the recognition of a large number of functional brain networks reconstructed by a sparse representation of whole-brain fMRI signals. The 3D CNN on the other hand extracts 3D spatial features from the 4D volumetric and could potentially overlook 3D structure information [60]. Although CNN can share the filter in the convolving layer and the number of parameters can be reduced in the pooling layer, the large amount of data required by the 3D network still demands extended training time [41].

In our approaches, we incorporated 5-layer convolution residual blocks on the brain ROI BOLD signals data [32].

In each residual block, the first convolutional layer used 1×1 convolutional filters to reduce the time dimension down to 3 and generate temporal descriptors for each voxel of the volume of the fMRI. Then followed by 1×3 and 3×1 blocks to replace a single 3×3 layer while reducing half of the parameters. The convolutional and residual blocks are then stacked to extract the high-level 2D signal features. Then decode multiple brain task states from fMRI signals from the Local Connectivity and compositionality of image data [55]. The series of convolutional and residual blocks will lead dimension could be quickly reduced and finally flatten to 64 features and performed classification.

D. Dynamic Temporal Feature Extraction

Mainly, the "deep in space" (CNN) and the "deep in time" (RNN) network are two deep learning branches. It is natural to use CNN on the standard grid-like brain images and use RNN for sequence classification. However, CNN due to its emphasis on the spatial relationship on the localized data, it neglects the information on the temporal domain which entails a significant amount of information.

Instead of using functional connectivity or spatial maps as input, RNN models fully capitalize on the dynamic time courses directly. LSTM is a special model based on RNN that can effectively solve the problem of long-term dependence by several gateways that fit into the brain of fMRI changes associated with voxels along with time series.

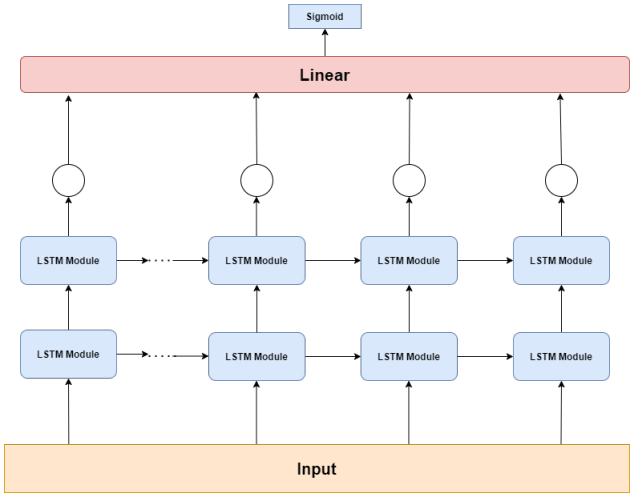

Fig. 9: Our implementation of 2 layer LSTM followed by a dense layer of single nodes

Hence, after experimenting with the CNN architecture, we decided to explore the effectiveness of a temporal model instead. We utilized the work of Dvornek etal(2017) as a reference, where the LSTM takes the resting-state fMRI time-series as the input and direct the output of LSTM module to a dense layer of singles nodes(Figure 9)[11]. As this architecture is suggested to give each time point more direct weighting in the result instead of the conventional where only the final output of the sequence is considered[11]. Consequently, this should be able to exhibit a higher resistance against inevitable noises from the fMRI data.

Even though the LSTM model yields a promising result of 73.88% accuracy on the raw data using the MSDL mask, there is still room for improvement. Referring to the treatise, El-Gazzar1 ec al [13] proposed a convolutional neural network with 3D LSTM to account for the spatiotemporal features from the full 4D fMRI data, Yan et al. [57] combined the CNN and GRU by extracting the temporal feature via CNN before feeding into the Gated Recurrent Unit. These examples demonstrated the possibility to combine the 2 architecture to yield a better result. Unlike El-Gazzarl et al. and Yan et al. used CNN to extract spatial features, we applied a CONV1D layer after LSTM to extract the temporal information to a greater extent (Fig 10). Max pooling layer is also added after CONV1D to condense the data to a deeper extent for the linear network.

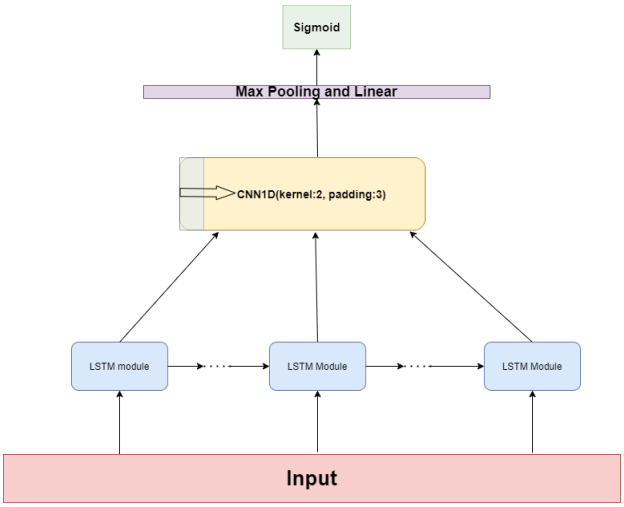

Fig. 10: Hybrid model of CNN and LSTM

E. Graph Methods

The methods implemented and illustrated above focus on either euclidean or temporal domain of the 4D volumetric fMRI data on. In this section, we provide a different data representation on the non-euclidean domain, by extracting high-level node representations and therefore to obtain compact manifolds on the brain connectivity graphs [55].

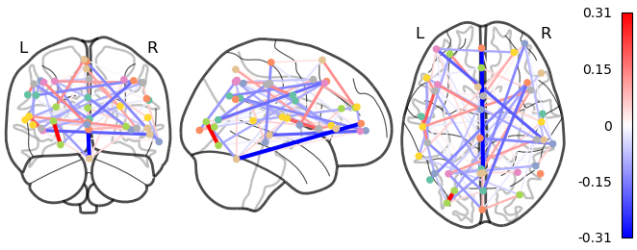

Fig. 11: The connection between brain atlases

The graph construction from 4D fMRI image is based on the fact that the brain atlas are interconnected in an undirected manner, this is emphasized through the functional connectivity matrix shown in figure 5, where it is seen as a graph representation named adjacency matrix with each grid representing the potential weighted linkage between brain atlas. The correlation scores for each linkage highlights the strength of the connection. The visualizations of the graph constructed from the correlations matrix can be found in Fig. 11 [26], [42], [38].

Based on this graph construction, the network embedding aims at representing network nodes as low-dimensional vector representations, while preserving both network topology structure and node content information. Some typical graph measures highlighted in recent literature including, nodal degree, local efficiency and betweenness centrality, shortest path, clustering coefficient and k coreness centrality etc [35], [29], [27]. These graph embeddings summarise the graph representations globally and locally, and then these embeddings are used for encoding the graph shown in 12.

The graph embedding is effective, however, it cannot aggregate information to monitor the dynamic change on the node level. The GCN (Graph Convolutional Neural Network) directly performs graph convolution operation based on the extracted graph representations and therefore are much more efficient at mapping graph dynamics [23]. The convolutional layer in GCN aggregates the information from neighbours and passes the message recursively to aggregate its node embeddings. The graph is then processed using pooling layers to reduce the size either by grouping the nodes or pruning the original graph to a subgraph [55], [59]. Then the readout layer to summarise the embedded graph representation in vectorized form and then fed into the classifier for graph level classification.

In particular the graph convolution operation is shown in Equation 1. The notations defines the graph adjacency matrix $\widetilde{A}$ and normalized nodal degrees $\widetilde{D}$. The θ in the equation is the learnable weights updated by the neural networks and σ is the activation function that increases the non-linearity (e.g. tanh, ReLU). This graph convolution is illustrated in 12 the node states at layer h^{l+1} are determined by the previous state h^l with convolve the neighbour state, the aggregated messages are passed throughout the entire graph [23].

$$h^{l+1} = \sigma(\widetilde{D}^{-\frac{1}{2}}\widetilde{A}\widetilde{D}^{-\frac{1}{2}}h^l\theta) \tag{1}$$

We further incorporate attention mechanism, a spatial approach to implicitly compute the convolutions directly on the graph to learn distinctive weights of nodes in their neighborhoods [51], [45], [49]. The detailed equation is shown in equation 2, where the hidden state summing the neighbourhood message with a recomputed attention score α_{ij}. This attention score α_{ij} is the attention coefficeint computed the softmax connection weights in the neighbour subgraphs. In other words, the network can explicitly map the weighted

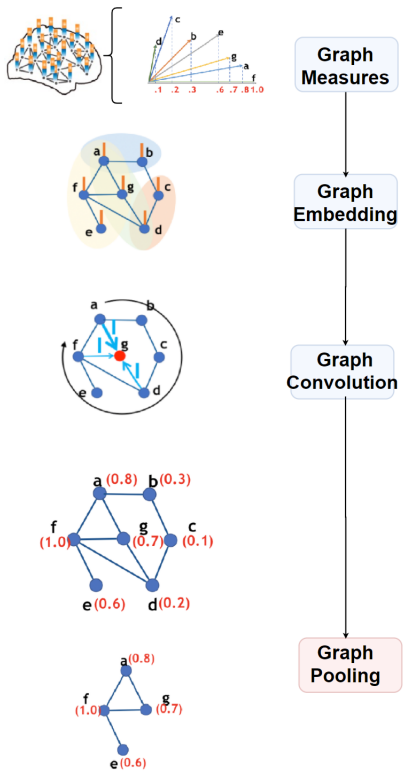

Fig. 12: The graph convolution layer

importance of its neighbour connections.

$$h^{l+1} = \sigma(\frac{1}{K}\sum_{k=1}^{K}\sum_{j\in N_i}\alpha_{ij}^k W^k \widetilde{h_j}^l) \tag{2}$$

After updated the node state, we can further extract the graph latent space using graph pooling, and reduce the size of the graph [25], [45]. In this report, we incorporated an attention-based pooling technique called self-attention graph (SAG) pooling [25]. The key idea is to use the convolution layer to compute self-attention scores and used it as a threshold to remove nodes. The top N nodes are selected to be kept based on the convoluted scores and a specified pooling ratio of $k \in (0, 1]$. The updated adjacency matrix using SAG pooling can be expressed in 3 and the Fig. 12.

$$Z_{Mask} = topN(h^l), X = X \odot Z_{Mask} \tag{3}$$

To extract the and perform graph level classification on the defined task. We incorporated the aforementioned techniques along with skip connection [15], the detailed architecture can be shown in Fig. 12. The proposed architecture is constructed using three convolution layers with attention mechanism and SAG pooling, each linked using skip connection. Additionally, to compare the mode performance of we also introduced a baseline GCN model with 3-layer convolutions and global pooling. Techniques such as random edge dropout are also applied after each convolution layer [39].

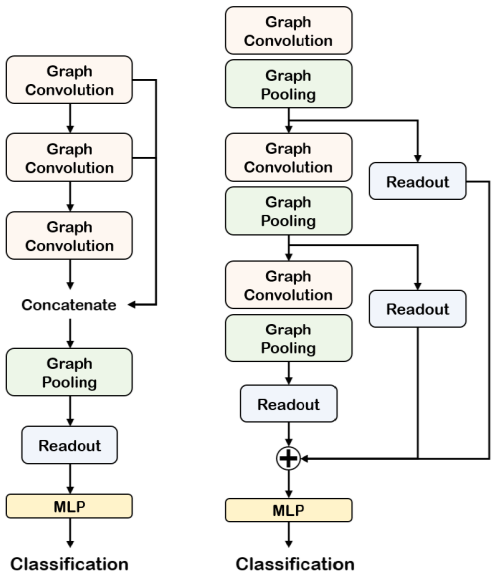

Fig. 13: The graph convolution [25]

F. Ensemble model

Ensemble model can be constructed in two different ways through either brain atlases or classifier models. In [24], classifiers including SVM are ensembled for better accuracy. On the other hand, we tried a different approach in this project by ensembling different atlas scheme. To be more specific, MSDL, AAL, Harvord-Oxford and Ward-clustering-based ROIs are fed into multiple deep learning model with a same structure respectively, and then the results are connected into a multi layer perceptron model to produce the result.

V. Experiments and Results

A. Data Acquisition

Alzheimer's Disease Neuroimaging Initiative (ADNI), is a public repository launched in 2011 containing images and clinical data from 2000+ human datasets over different projects and data modalities specialising Alzheimer's Disease [1]. The brain images are categorized into 4 primary labelled classes,

1) Alzheimer's Disease (AD): Patients in this category has been diagnosed with progressive dementia and memory deficit (AD). [16]
2) Cognitively Normal (CN): Patients are labelled as clinically normal.
3) Mild Cognitive Disorder (MCI): Patients in this category are commonly characterized by slight cognitive disorder but largely intact of daily activities.
   Approximately 10–15% of individuals with MCI tend to progress to AD [44]. MCI can be further divided into Early Mild Cognitive Disorder (EMCI) and Late Mild Cognitive Disorder (LMCI) according to the extent of episodic memory impairment and risk of conversion to AD [16], [58].
4) Subjective Memory Concerns (SMC): stated the intermediate state in transitioning from MCI to early stage [8].

In our experiments, 273 total fMRI subjects were obtained from ADNI dataset, with 92 subjects of AD, 130 subjects of CN, 46 subjects of MCI and 8 subjects of SMC, highlighted in I. The number distribution of each class is shown in Fig. 14.

Class	Count
AD	92
CN	130
MCI	46
SMC	8
Total	**273**

TABLE I: Data class summarize

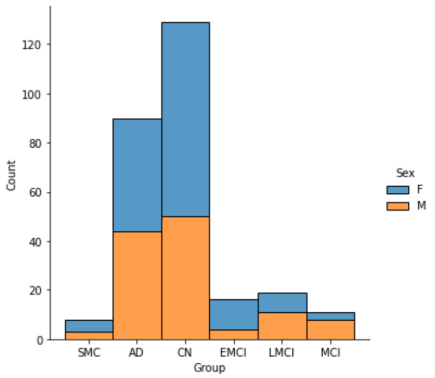

Fig. 14: Data explore on female and male

The metadata of ADNI brain images also consists of age and gender labels for the individual subject. This allows us to pre-explore the insights via exploratory data analysis. As the Fig. 15 shown, our data collection has patients with an age range from 46 to 105 years old, follows Gaussian distribution with a mean approximately 75 years old for both genders. However, it is also observed in Fig. 14, the number of subjects for each class is not balanced. Since our data collection is relatively small and the class labels are heavily relying on the human definition. To handle such class imbalance problem while conforming the underlying clinical definition, we re-allocated the labels into cognitively impaired (CI) and cognitively normal (CN) [8]. The dataset after merging MCI, AD and SMC into cognitively impaired (CI) have shown obtaining a balancing number as shown in 15. This data collection is then used in our experiments for training and evaluating the model performance.

B. Experiments and results

In this section, We examine the aforementioned methods using quantitative analysis with selected parcellation schemes, including AAL, MSDL, Harvard Oxford and ICA in section V-B1. We also explore the insight of the neural network models and interpret the results in section V-B2. We performed preprocessing steps on the data and augmentation method

Fig. 15: EDA age

demonstrated in previous sections and transform using different ROIs to testify deep learning models including,

1) SVM as a baseline machine learning model.
2) 2-layer perceptron as a deep learning baseline model.
3) A 2 dimensional CNN with 5 residual blocks.
4) 2-layer standard LSTM with hidden size 64
5) 1 layer LSTM layer followed by 1D CNN to generate temporal descriptor for each ROI signal.
6) 3 layer GCN with skip connection and global pooling
7) 3 layer Graph attentional network with SAG pooling based on methods suggested in [25].

For each model, we conducted a comprehensive grid search for optimal hyper-parameters and 5-fold cross-validation to reassure the reliability of results. The results and the parameters from intermediate layers in the neural networks are withdrawn for further interpretation in section V-B2. All models are written in Python and using Pytorch (https://pytorch.org) and the complete project code is available at GitHub (https://github.com/floracitrus/P-NP).

1) Quantitative Results: The hyperparameter tuning is completed using Ray (https://docs.ray.io) aiming to find the best learning rate, weight decay and using CrossEntropy Loss with 0.0005 learning rate with Adam optimizer over 1000 epochs of training [22]. The detailed test results are illustrated in Table II. Since the training of ensemble ROIs collapses and the weight of each branch was not updated appropriately, the results of ensemble models are not considered. As the results highlighting the LSTM-CNN outperformed the other architecture based on accuracy. However, the overall results have shown a relative low accuracy score. We will have further discussion in Section VI.

2) Qualitative Results: To visualize the outputs and explain the biomarkers, we chose the best performed LSTM-CNN model and the GAT-SAG to interpret the parameters at each layer to peek the insights of neural networks.

After the training is completed, we extracted the parameters from the input and the output layer of LSTM-CNN. Then compare qualitatively using dimension techniques named t-SNE [31]. The figure 16 shows the t-SNE projection of input and output parameters on 2d space. It can be observed that the input signal data is not separable, however, after encoding by LSTM-CNN the projections shown as red and blue dots are differentiable by inspection. This supports the capability of LSTM-CNN in transforming high-dimensional brain signal data to high-level distinguishable data. Due to the nature of

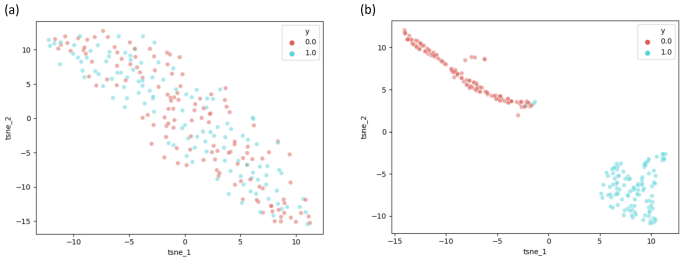

Fig. 16: The tSNE projection of the hidden parameters of the input layer in the LSTM model shown in (a) and the fully connected layer shown in (b)

graph neural networks map the interconnections between brain atlases, it is also capable of locating the most characteristic ROIs, we can then interpret the layers in GCN model despite the poor performance on brain imaging classification.

Since the input of the graph neural network is the adjacency matrix with corresponding node embeddings and edge weights, we can then map the evolving graph on the brain scale and tracks the dynamic signal flows through individual ROIs. This is shown in Fig 17, reflected by the colour and the intensity of each node. Comparatively, each pair of figures such as fig 17a and 17c conveys the changes in reducing less relevant and discriminative nodes and edges.

We chose MSDL network since it has fewer number of ROIs (39), the resultant visualizations in 17 have shown the most significant brain community that contributes to the cognitive problem. For example, the **default mode network** (DMN) networks proposed in [48], consists of vortex such as posterior cingulate cortex/precuneus and angular gyrus. It is also proven in recent studies that patients with cognitive disorder have a reduction in glucose in the DMN related vortex [2], [6]. This confirms our hypothesis of DMN atlas that is explained by the graph neural network.

VI. Discussion

The overall accuracy score revealed in table II cannot provide a solid conclusion of which model outperforms in classifying cognitive disorder patients. The results rendered by the implemented methods are still not ideal. Due to time constraints, we cannot explore this problem further, but in this section, we summarise the main potential reasons that may

TABLE II: Performance of different models

Method	AAL (116 ROIs)			MSDL (39 ROIs)			Harvard Oxford (48 ROIs)			ICA Selected (50 ROIs)
	Raw	Sliding Window	Interpolation	Raw	Sliding Window	Interpolation	Raw	Sliding Window	Interpolation	Raw
SVM	72.72	-	-	68.36	-	-	73.09	-	-	-
MLP	70.73	68.29	53.37	73.17	53.65	55.84	71.80	68.83	58.32	50.9
CNN [ref]	53.66	60.97	57.88	46.34	60.16	52.13	43.90	62.67	61.22	60.97
RNN										
LSTM [ref]	71.35	58.87	56.28	73.88	60.97	60.75	64.35	67.82	62.35	58.67
LSTM-CNN	73.17	60.16	58.96	**75.61**	50.13	52.26	68.22	64.50	54.82	50.909
GNN										
GCN [ref]	58	56.82	50.30	52.27	60.61	42.31	54.55	64.96	52.48	-
GATConv + edge dropout	61.36	59.35	56.78	56.82	61.23	51.20	68.18	65.28	54.92	-

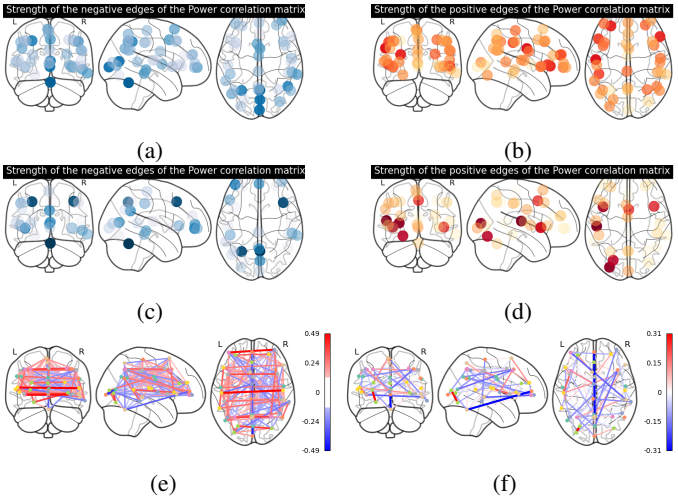

(a) (b) (c) (d) (e) (f)

Fig. 17: (a), (c) shows the raw signal strength for negative connection before and after GCN encoding, (b), (d) are the positive signal strength before and after GCN encoding. (e), (f) identifies the distinctive functional connectivity between brain ROIs before and after GNN encoding

be causing the poor performance and provide a discussion for future improvements.

A. Result

We have a very small dataset of only 273 subjects from ADNI, this is because the 4D fMRI image with the specified labels is hard to obtain from public datasets. The fMRI data is 4 dimensional and can be computationally heavy to be processed, large amount of confound can be captured during fMRI scanning and acquisition. These factors have increased the difficulties of perform common deep learning tasks on fMRI data. Although the we have examined a few data augmentation techniques to increase the size of dataset. However, this is still not helping to improve the model performance.

B. Model

In terms of the models we have implemented, common spectral and spatial techniques either neglect the functional dependency between different brain regions in a network or discard the information in the temporal dynamics of brain activity. Some recent studies proposed spatial-temporal methods [32], however, they are either computationally heavy or cannot be generalised into varying brain networks.

C. Functional connectivity

For further discussion on the input functional connectivity, in order to better capture the functional dynamics in the temporal domain, as well as to increase the sample size, we utilized the method called correlation of correlation. First we apply the data augmentation techniques with consecutive sliding window, then we will get an augmented time dimension T_{aug}, $T_{aug} < T$. Similarly, we flatten the functional dynamics $(N*(\frac{1}{2}*M*M)*T_{aug})$. Then we cluster based on 273 subjects and then group the flattened functional connectivity and reduce them to a much smaller number C. Next we run correlation on (N, C, T_{aug}), and get the correlation as (N, C, C) then finally we flatten it to $(N, (\frac{1}{2} * C * C))$ as input to gcn, nn, lstm. However the tested accuracy didn't improve much through this method.

D. Community detection

As discussed in the results section, we had extracted a GCN layer in order to find out the communities for community detection. This can be accomplished more accurately through the application of a mathematical modelling technique known as *Poisson Stochastic Block Modeling*. This model is inspired from the latent communities detection in social science [10]. Stochastic block model is an idea of grouping the instances in the network by node [37], and Homogeneous Poisson process is the most common counting process model. It could be defined as a random process in which each event occurs independently at a rate per unit time.

If we viewed it as a graph problem, we can treat ROIs as nodes, functional connectivity threshold $> c$ as an edge, and along the augmented data time domain, when there an edge appears at a certain time-stamp, we count it as one event arrival and record the interaction nodes. The behaviour of the group of nodes is influenced by the community they belong to. Thus the functional connectivity between any two clustered ROI groups is obeying the Poisson process. This implies that instead of building a clustering model based only on the edges between individuals, we model the instances that belong to certain groups and which interact following a certain pattern. Then we used the Bayesian model with efficient Gibbs sampling method to sample the group assignment and the event intensity. To extend it further, we can assume they obey

Hawkes process rather than Poisson process to capture the self-exciting characteristic, however we didn't have time to test the Hawkes model. The Poisson stochastic block model when we are trying to assign AAL atlas to 10 groups shows. The 10 groups interaction intensity is seen in fig 18.

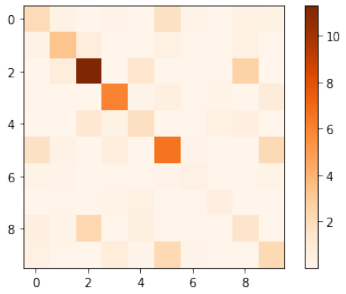

Fig. 18: Event arrival intensity plot

An example AAL ROI clustering is shown as figure 19, where the cylinder contains the index of ROI which can be treated as a same group by the intensity of functional connectivity. The λ_{ij} corresponding the event intensity between group i to j reflected in figure 18.

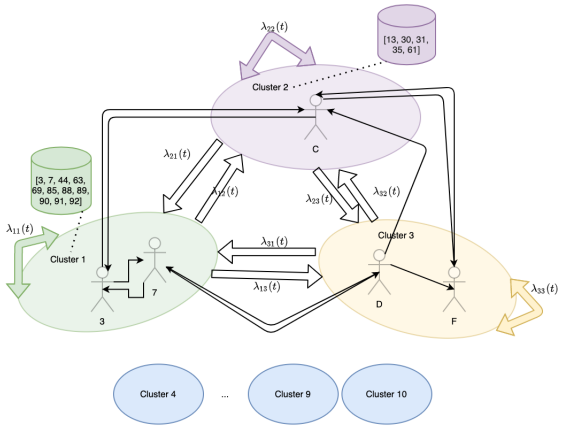

Fig. 19: Poisson stochastic block model result

However in this method, there are two values we need to prefix, the number of communities we would like to find and the threshold of functional connectivity which we treated as an edge. Thus this adds more uncertainty on the model itself. In Bayesian setting, if we apply the Chinese Restaurant Process as the group assignment prior, we then have no need to fix the number of communities we would like to find, but the threshold value still remains on testing. This can be the potential input for the Neural networks and potentially improve the result.

VII. Conclusion

In this paper, we explored various deep learning approaches to solve the problem of clinical diagnoses of cognitive impairment patients based on resting-state functional magnetic resonance images. We performed data processing on fMRI images obtained from the ADNI database, including normalization, motion correction and confound regression. Dividing the data into two discrete groups: Cognitive Normal (CN) and Cognitive Impaired (CI) including patients with AD, MCI and SMC. We implemented new methods with ensemble learning and graph neural networks. Although the result didn't improve from the previous, this provides a future direction for further studies. The implemented methods identified the distinctive sets of the brain and explained informative biomarkers regarding deficit brain functional nodes.

References

[1] *ADNI — Alzheimer's Disease Neuroimaging Initiative*. URL: http://adni.loni.usc.edu/ (visited on 09/07/2020).

[2] Jessica R. Andrews-Hanna, Jonathan Smallwood, and R. Nathan Spreng. "The default network and self-generated thought: component processes, dynamic control, and clinical relevance". In: *Annals of the New York Academy of Sciences* 1316.1 (May 2014), pp. 29–52. ISSN: 0077-8923. DOI: 10.1111/nyas.12360. URL: https://www.ncbi.nlm.nih.gov/pmc/articles/PMC4039623/ (visited on 12/08/2020).

[3] John Ashburner and Karl J. Friston. "Unified segmentation". en. In: *NeuroImage* 26.3 (July 2005), pp. 839–851. ISSN: 10538119. DOI: 10.1016/j.neuroimage.2005.02.018. URL: https://linkinghub.elsevier.com/retrieve/pii/S1053811905001102 (visited on 12/07/2020).

[4] Iman Beheshti et al. "Structural MRI-based detection of Alzheimer's disease using feature ranking and classification error". en. In: *Computer Methods and Programs in Biomedicine* 137 (Dec. 2016), pp. 177–193. ISSN: 01692607. DOI: 10.1016/j.cmpb.2016.09.019. URL: https://linkinghub.elsevier.com/retrieve/pii/S0169260716301055 (visited on 12/07/2020).

[5] Colin J. Brown and Ghassan Hamarneh. "Machine Learning on Human Connectome Data from MRI". en. In: *arXiv:1611.08699 [cs, q-bio, stat]* (Nov. 2016). arXiv: 1611.08699. URL: http://arxiv.org/abs/1611.08699 (visited on 05/17/2020).

[6] Randy L. Buckner, Jessica R. Andrews-Hanna, and Daniel L. Schacter. "The brain's default network: anatomy, function, and relevance to disease". eng. In: *Annals of the New York Academy of Sciences* 1124 (Mar. 2008), pp. 1–38. ISSN: 0077-8923. DOI: 10.1196/annals.1440.011.

[7] J. -. Cardoso. "Blind signal separation: statistical principles". In: *Proceedings of the IEEE* 86.10 (1998), pp. 2009–2025. DOI: 10.1109/5.720250.

[8] Young Min Choe et al. *Subjective memory complaint as a useful tool for the early detection of Alzheimer’s disease*. English. Journal Abbreviation: NDT Pages: 2451-2460 Publisher: Dove Press Volume: 14. Sept. 2018. DOI: 10.2147/NDT.S174517. URL: https://www.dovepress.com/subjective-memory-

complaint-as-a-useful-tool-for-the-early-detection-o-peer-reviewed-article-NDT (visited on 12/06/2020).

[9] Corinna Cortes and Vladimir Vapnik. "Support-vector networks". en. In: *Machine Learning* 20.3 (Sept. 1995), pp. 273–297. ISSN: 1573-0565. DOI: 10.1007/BF00994018. URL: https://doi.org/10.1007/BF00994018 (visited on 12/07/2020).

[10] Christopher DuBois, Carter T Butts, and Padhraic Smyth. "Stochastic blockmodeling of relational event dynamics". en. In: (), p. 9.

[11] Nicha C. Dvornek et al. "Identifying Autism from Resting-State fMRI Using Long Short-Term Memory Networks". In: *Machine Learning in Medical Imaging*. Ed. by Qian Wang et al. Vol. 10541. Series Title: Lecture Notes in Computer Science. Cham: Springer International Publishing, 2017, pp. 362–370. ISBN: 978-3-319-67388-2 978-3-319-67389-9. DOI: 10.1007/978-3-319-67389-9_42. URL: http://link.springer.com/10.1007/978-3-319-67389-9_42 (visited on 09/08/2020).

[12] Rachael Garner et al. "A Machine Learning Model to Predict Seizure Susceptibility from Resting-State fMRI Connectivity". In: *2019 Spring Simulation Conference (SpringSim)*. Tucson, AZ, USA: IEEE, Apr. 2019, pp. 1–11. ISBN: 978-1-5108-8388-8. DOI: 10.23919/SpringSim.2019.8732859. URL: https://ieeexplore.ieee.org/document/8732859/ (visited on 05/21/2020).

[13] Ahmed El-Gazzar et al. "A Hybrid 3DCNN and 3DC-LSTM based model for 4D Spatio-temporal fMRI data: An ABIDE Autism Classification study". en. In: *arXiv:2002.05981 [cs]* (Feb. 2020). arXiv: 2002.05981. URL: http://arxiv.org/abs/2002.05981 (visited on 12/04/2020).

[14] Cyril Goutte et al. "On Clustering fMRI Time Series". In: *NeuroImage* 9.3 (1999), pp. 298–310. ISSN: 1053-8119. DOI: https://doi.org/10.1006/nimg.1998.0391. URL: http://www.sciencedirect.com/science/article/pii/S1053811998903913.

[15] Kaiming He et al. "Deep Residual Learning for Image Recognition". In: *arXiv:1512.03385 [cs]* (Dec. 2015). arXiv: 1512.03385. URL: http://arxiv.org/abs/1512.03385 (visited on 12/07/2020).

[16] Frank Jessen et al. "AD dementia risk in late MCI, in early MCI, and in subjective memory impairment". In: *Alzheimer's & Dementia* 10.1 (2014), pp. 76–83. ISSN: 1552-5260. DOI: https://doi.org/10.1016/j.jalz.2012.09.017. URL: http://www.sciencedirect.com/science/article/pii/S1552526012025782.

[17] C Jongkreangkrai et al. "Computer-aided classification of Alzheimer's disease based on support vector machine with combination of cerebral image features in MRI". In: *Journal of Physics: Conference Series* 694 (Mar. 2016), p. 012036. ISSN: 1742-6588, 1742-6596. DOI: 10.1088/1742-6596/694/1/012036. URL: https://iopscience.iop.org/article/10.1088/1742-6596/694/1/012036 (visited on 12/07/2020).

[18] Sandhya Joshi et al. "Classification of Alzheimer's Disease and Parkinson's Disease by Using Machine Learning and Neural Network Methods". In: *2010 Second International Conference on Machine Learning and Computing*. Bangalore: IEEE, Feb. 2010, pp. 218–222. ISBN: 978-1-4244-6006-9 978-1-4244-6007-6. DOI: 10.1109/ICMLC.2010.45. URL: https://ieeexplore.ieee.org/document/5460738/ (visited on 12/07/2020).

[19] Justin Ker et al. "Deep Learning Applications in Medical Image Analysis". In: *IEEE Access* 6 (2018), pp. 9375–9389. ISSN: 2169-3536. DOI: 10.1109/ACCESS.2017.2788044. URL: http://ieeexplore.ieee.org/document/8241753/ (visited on 05/31/2020).

[20] Ali Khazaee, Ata Ebrahimzadeh, and Abbas Babajani-Feremi. "Application of advanced machine learning methods on resting-state fMRI network for identification of mild cognitive impairment and Alzheimer's disease". en. In: *Brain Imaging and Behavior* 10.3 (Sept. 2016), pp. 799–817. ISSN: 1931-7557, 1931-7565. DOI: 10.1007/s11682-015-9448-7. URL: http://link.springer.com/10.1007/s11682-015-9448-7 (visited on 05/13/2020).

[21] Meenakshi Khosla et al. "Ensemble learning with 3D convolutional neural networks for connectome-based prediction". en. In: *arXiv:1809.06219 [cs, stat]* (June 2019). arXiv: 1809.06219. URL: http://arxiv.org/abs/1809.06219 (visited on 05/13/2020).

[22] Diederik Kingma and Jimmy Ba. "Adam: A Method for Stochastic Optimization". In: *International Conference on Learning Representations* (Dec. 2014).

[23] Thomas N Kipf and Max Welling. "Semi-Supervised Classification with Graph Convolutional Network". en. In: (2017), p. 14.

[24] Ludmila I. Kuncheva and Juan J. Rodríguez. "Classifier ensembles for fMRI data analysis: an experiment". eng. In: *Magnetic Resonance Imaging* 28.4 (May 2010), pp. 583–593. ISSN: 1873-5894. DOI: 10.1016/j.mri.2009.12.021.

[25] Junhyun Lee, Inyeop Lee, and Jaewoo Kang. "Self-Attention Graph Pooling". In: *arXiv:1904.08082 [cs, stat]* (June 2019). arXiv: 1904.08082. URL: http://arxiv.org/abs/1904.08082 (visited on 09/20/2020).

[26] Xiaoxiao Li et al. *BrainGNN: Interpretable Brain Graph Neural Network for fMRI Analysis*. en. preprint. Neuroscience, May 2020. DOI: 10.1101/2020.05.16.100057. URL: http://biorxiv.org/lookup/doi/10.1101/2020.05.16.100057 (visited on 07/30/2020).

[27] Xiaoxiao Li et al. "Graph Embedding Using Infomax for ASD Classification and Brain Functional Difference Detection". In: *arXiv:1908.04769 [cs, eess, stat]* (Aug. 2019). arXiv: 1908.04769. URL: http://arxiv.org/abs/1908.04769 (visited on 05/31/2020).

[28] Geert Litjens et al. "A survey on deep learning in medical image analysis". en. In: *Medical Image Analysis* 42 (Dec. 2017), pp. 60–88. ISSN: 13618415. DOI: 10.1016/j.media.2017.07.005. URL: https://linkinghub.

elsevier.com/retrieve/pii/S1361841517301135 (visited on 05/31/2020).

[29] Ye Liu et al. "Multi-View Multi-Graph Embedding for Brain Network Clustering Analysis". en. In: (), p. 8.

[30] Gill Livingston et al. "Dementia prevention, intervention, and care: 2020 report of the Lancet Commission". en. In: *The Lancet* 396.10248 (Aug. 2020), pp. 413–446. ISSN: 01406736. DOI: 10.1016/S0140-6736(20)30367-6. URL: https://linkinghub.elsevier.com/retrieve/pii/S0140673620303676 (visited on 12/06/2020).

[31] Laurens van der Maaten and Geoffrey Hinton. "Visualizing Data using t-SNE". In: *Journal of Machine Learning Research* 9 (2008), pp. 2579–2605. URL: http://www.jmlr.org/papers/v9/vandermaaten08a.html.

[32] Zhenyu Mao et al. "Spatio-temporal deep learning method for ADHD fMRI classification". en. In: *Information Sciences* 499 (Oct. 2019), pp. 1–11. ISSN: 00200255. DOI: 10.1016/j.ins.2019.05.043. URL: https://linkinghub.elsevier.com/retrieve/pii/S0020025519304475 (visited on 09/01/2020).

[33] M. J. McKeown et al. "Analysis of fMRI data by blind separation into independent spatial components". eng. In: *Human Brain Mapping* 6.3 (1998), pp. 160–188. ISSN: 1065-9471. URL: https://www.ncbi.nlm.nih.gov/pmc/articles/PMC6873377/.

[34] Martin J McKeown, Lars Kai Hansen, and Terrence J Sejnowski. "Independent component analysis of functional MRI: what is signal and what is noise?" In: *Current opinion in neurobiology* 13.5 (Oct. 2003), pp. 620–629. ISSN: 0959-4388. URL: https://www.ncbi.nlm.nih.gov/pmc/articles/PMC2925426/ (visited on 12/08/2020).

[35] Lu Meng and Jing Xiang. "Brain Network Analysis and Classification Based on Convolutional Neural Network". en. In: *Frontiers in Computational Neuroscience* 12 (Dec. 2018), p. 95. ISSN: 1662-5188. DOI: 10.3389/fncom.2018.00095. URL: https://www.frontiersin.org/article/10.3389/fncom.2018.00095/full (visited on 05/31/2020).

[36] Kevin Murphy, Rasmus M. Birn, and Peter A. Bandettini. "Resting-state FMRI confounds and cleanup". In: *NeuroImage* 80 (Oct. 2013), pp. 349–359. ISSN: 1053-8119. DOI: 10.1016/j.neuroimage.2013.04.001. URL: https://www.ncbi.nlm.nih.gov/pmc/articles/PMC3720818/ (visited on 06/21/2020).

[37] M. E. J. Newman and M. Girvan. "Finding and evaluating community structure in networks". In: *Physical Review E* 69.2 (Feb. 2004). arXiv: cond-mat/0308217, p. 026113. ISSN: 1539-3755, 1550-2376. DOI: 10.1103/PhysRevE.69.026113. URL: http://arxiv.org/abs/cond-mat/0308217 (visited on 11/07/2020).

[38] Himanshu Padole, S.D. Joshi, and Tapan K. Gandhi. "Early Detection of Alzheimer's Disease using Graph Signal Processing on Neuroimaging Data". In: *2018 2nd European Conference on Electrical Engineering and Computer Science (EECS)*. Bern, Switzerland: IEEE, Dec. 2018, pp. 302–306. ISBN: 978-1-72811-929-8. DOI: 10.1109/EECS.2018.00062. URL: https://ieeexplore.ieee.org/document/8910066/ (visited on 06/18/2020).

[39] Yu Rong et al. "DropEdge: Towards Deep Graph Convolutional Networks on Node Classification". en. In: Sept. 2019. URL: https://openreview.net/forum?id=Hkx1qkrKPr (visited on 12/07/2020).

[40] Alex Novaes Santana et al. "Using Deep Learning and Resting-State fMRI to Classify Chronic Pain Conditions". en. In: *Frontiers in Neuroscience* 13 (Dec. 2019), p. 1313. ISSN: 1662-453X. DOI: 10.3389/fnins.2019.01313. URL: https://www.frontiersin.org/article/10.3389/fnins.2019.01313/full (visited on 05/13/2020).

[41] S. Sarraf and G. Tofighi. "Deep learning-based pipeline to recognize Alzheimer's disease using fMRI data". In: *2016 Future Technologies Conference (FTC)*. 2016, pp. 816–820. DOI: 10.1109/FTC.2016.7821697.

[42] Tzu-An Song et al. "Graph Convolutional Neural Networks For Alzheimer's Disease Classification". en. In: *2019 IEEE 16th International Symposium on Biomedical Imaging (ISBI 2019)*. Venice, Italy: IEEE, Apr. 2019, pp. 414–417. ISBN: 978-1-5386-3641-1. DOI: 10.1109/ISBI.2019.8759531. URL: https://ieeexplore.ieee.org/document/8759531/ (visited on 08/02/2020).

[43] Ryo Takahashi, Takashi Matsubara, and Kuniaki Uehara. "Data Augmentation Using Random Image Cropping and Patching for Deep CNNs". en. In: *IEEE Transactions on Circuits and Systems for Video Technology* 30.9 (Sept. 2020), pp. 2917–2931. ISSN: 1051-8215, 1558-2205. DOI: 10.1109/TCSVT.2019.2935128. URL: https://ieeexplore.ieee.org/document/8795523/ (visited on 12/05/2020).

[44] M. Tanveer et al. "Machine Learning Techniques for the Diagnosis of Alzheimer's Disease: A Review". In: *ACM Transactions on Multimedia Computing, Communications and Applications* 16 (Apr. 2020), p. 35. DOI: 10.1145/3344998.

[45] Kiran K. Thekumparampil et al. "Attention-based Graph Neural Network for Semi-supervised Learning". en. In: (Mar. 2018). URL: https://arxiv.org/abs/1803.03735v1 (visited on 08/31/2020).

[46] Bertrand Thirion et al. "Which fMRI clustering gives good brain parcellations?" English. In: *Frontiers in Neuroscience* 8 (2014). ISSN: 1662-453X. DOI: 10.3389/fnins.2014.00167. URL: https://www.frontiersin.org/articles/10.3389/fnins.2014.00167/full (visited on 12/08/2020).

[47] N. Tzourio-Mazoyer et al. "Automated Anatomical Labeling of Activations in SPM Using a Macroscopic Anatomical Parcellation of the MNI MRI Single-Subject Brain". en. In: *NeuroImage* 15.1 (Jan. 2002), pp. 273–289. ISSN: 1053-8119. DOI: 10.1006/nimg.2001.0978. URL: http://www.sciencedirect.com/science/article/pii/S1053811901909784 (visited on 12/08/2020).

[48] Gaël Varoquaux and R. Cameron Craddock. "Learning and comparing functional connectomes across subjects". en. In: *NeuroImage* 80 (Oct. 2013), pp. 405–415. DOI: 10.1016/j.neuroimage.2013.04.007. URL: https://hal.inria.fr/hal-00812911 (visited on 12/08/2020).

[49] Ashish Vaswani et al. "Attention is All you Need". en. In: (), p. 11.

[50] Dallas P. Veitch et al. "Understanding disease progression and improving Alzheimer's disease clinical trials: Recent highlights from the Alzheimer's Disease Neuroimaging Initiative". en. In: *Alzheimer's & Dementia* 15.1 (Jan. 2019), pp. 106–152. ISSN: 15525260. DOI: 10.1016/j.jalz.2018.08.005. URL: http://doi.wiley.com/10.1016/j.jalz.2018.08.005 (visited on 12/06/2020).

[51] Petar Veličković et al. "Graph Attention Networks". en. In: *arXiv:1710.10903 [cs, stat]* (Feb. 2018). arXiv: 1710.10903. URL: http://arxiv.org/abs/1710.10903 (visited on 08/31/2020).

[52] Manasij Venkatesh, Joseph Jaja, and Luiz Pessoa. "Comparing functional connectivity matrices: A geometry-aware approach applied to participant identification". In: *NeuroImage* 207 (2020), p. 116398. ISSN: 1053-8119. DOI: https://doi.org/10.1016/j.neuroimage.2019.116398. URL: http://www.sciencedirect.com/science/article/pii/S1053811919309899.

[53] Xiaoxiao Wang et al. "Decoding and mapping task states of the human brain via deep learning". en. In: *Human Brain Mapping* 41.6 (Apr. 2020), pp. 1505–1519. ISSN: 1065-9471, 1097-0193. DOI: 10.1002/hbm.24891. URL: https://onlinelibrary.wiley.com/doi/abs/10.1002/hbm.24891 (visited on 05/13/2020).

[54] Susan Whitfield-Gabrieli and Alfonso Nieto-Castanon. "Conn: A Functional Connectivity Toolbox for Correlated and Anticorrelated Brain Networks". en. In: *Brain Connectivity* 2.3 (June 2012), pp. 125–141. ISSN: 2158-0014, 2158-0022. DOI: 10.1089/brain.2012.0073. URL: http://www.liebertpub.com/doi/10.1089/brain.2012.0073 (visited on 07/05/2020).

[55] Zonghan Wu et al. "A Comprehensive Survey on Graph Neural Networks". In: *IEEE Transactions on Neural Networks and Learning Systems* (2020). arXiv: 1901.00596, pp. 1–21. ISSN: 2162-237X, 2162-2388. DOI: 10.1109/TNNLS.2020.2978386. URL: http://arxiv.org/abs/1901.00596 (visited on 06/10/2020).

[56] Maziar Yaesoubi, Tülay Adalı, and Vince D. Calhoun. "A window-less approach for capturing time-varying connectivity in fMRI data reveals the presence of states with variable rates of change". In: *Human Brain Mapping* 39.4 (Jan. 2018), pp. 1626–1636. ISSN: 1065-9471. DOI: 10.1002/hbm.23939. URL: https://www.ncbi.nlm.nih.gov/pmc/articles/PMC5847478/ (visited on 12/06/2020).

[57] Weizheng Yan et al. "Discriminating schizophrenia using recurrent neural network applied on time courses of multi-site FMRI data". en. In: *EBioMedicine* 47 (Sept. 2019), pp. 543–552. ISSN: 23523964. DOI: 10.1016/j.ebiom.2019.08.023. URL: https://linkinghub.elsevier.com/retrieve/pii/S2352396419305456 (visited on 06/18/2020).

[58] Tingting Zhang et al. "Classification of Early and Late Mild Cognitive Impairment Using Functional Brain Network of Resting-State fMRI". English. In: *Frontiers in Psychiatry* 10 (2019). Publisher: Frontiers. ISSN: 1664-0640. DOI: 10.3389/fpsyt.2019.00572. URL: https://www.frontiersin.org/articles/10.3389/fpsyt.2019.00572/full (visited on 12/06/2020).

[59] Ziwei Zhang, Peng Cui, and Wenwu Zhu. "Deep Learning on Graphs: A Survey". In: *arXiv:1812.04202 [cs, stat]* (Mar. 2020). arXiv: 1812.04202. URL: http://arxiv.org/abs/1812.04202 (visited on 06/10/2020).

[60] Yu Zhao et al. "Automatic Recognition of fMRI-derived Functional Networks using 3D Convolutional Neural Networks". In: *IEEE transactions on bio-medical engineering* 65.9 (Sept. 2018), pp. 1975–1984. ISSN: 0018-9294. DOI: 10.1109/TBME.2017.2715281. URL: https://www.ncbi.nlm.nih.gov/pmc/articles/PMC6146395/ (visited on 09/07/2020).

[61] A. B. Zonderman and G. A. Dore. "Risk of dementia after fluctuating mild cognitive impairment: When the yo-yoing stops". en. In: *Neurology* 82.4 (Jan. 2014), pp. 290–291. ISSN: 0028-3878, 1526-632X. DOI: 10.1212/WNL.0000000000000065. URL: http://www.neurology.org/cgi/doi/10.1212/WNL.0000000000000065 (visited on 12/08/2020).

[62] Arkan Al-Zubaidi et al. "Machine Learning Based Classification of Resting-State fMRI Features Exemplified by Metabolic State (Hunger/Satiety)". en. In: *Frontiers in Human Neuroscience* 13 (May 2019), p. 164. ISSN: 1662-5161. DOI: 10.3389/fnhum.2019.00164. URL: https://www.frontiersin.org/article/10.3389/fnhum.2019.00164/full (visited on 05/13/2020).